ELSEVIER

Journal of Molecular Catalysis A: Chemical 115 (1997) 329–338

JOURNAL OF MOLECULAR CATALYSIS A: CHEMICAL

Catalytic behavior of chromia and chromium-doped alumina pillared clay materials for the vapor phase deep oxidation of chlorinated hydrocarbons

Loretta Storaro [a], Renzo Ganzerla [a], Maurizio Lenarda [a,*], Roberto Zanoni [b], Antonio Jiménez López [c], Pascual Olivera-Pastor [c], Enrique Rodríguez Castellón [c]

[a] *Dipartimento di Chimica, Università di Venezia, D.D. 2137-30123 Venice, Italy*
[b] *Dipartimento di Chimica, Università di Roma (La Sapienza), Piazzale A. Moro 5, 00185 Rome, Italy*
[c] *Departamento de Química Inorgánica, Cristalografia y Mineralogía, Universidad de Málaga, Apdo. 59, 29071 Málaga, Spain*

Received 10 April 1996; revised 8 July 1996; accepted 8 July 1996

Abstract

The catalytic behavior of a chromium-doped alumina pillared clay (ACrPA) and a series of chromia-pillared clay materials (XSCr) for the deep oxidation of methylene chloride has been studied. Both types of catalysts showed a high activity (conversion > 80%) at $T > 350$°C. The ACrPA sample showed a virtually constant catalytic activity (conversion > 99%) in the 300–400°C temperature range while the activity of the XSCr samples markedly increased with the temperature reaching an almost total conversion at 400°C. XPS (X-ray photoelectron spectroscopy) and temperature programmed reduction (TPR) studies demonstrated that ACrPA is a Cr(VI)/Cr(III) mixed valence catalyst, whereas XSCr samples contain only chromium(III) ion. The high activity shown by ACrPA at low temperatures was attributed to the presence of highly dispersed Cr(VI) species, which exhibited an unusually high stability. The metal oxidation state of the two chromium based systems seemed to be important in determining the catalytic activity. The increase of the activity with the Cr content in XSCr samples suggested that the acid sites in these catalysts were located on the chromia pillars.

Keywords: Alumina; Chlorinated hydrocarbons; Chromia; CVOC; Oxidation; Pillared clays

1. Introduction

Chlorinated volatile compounds CVOCs (methylene chloride, trichloroethylene and carbon tetrachloride) constitute a major portion of the hazardous solvent wastes produced by industry and the major source of air pollution [1], so in many cases, legislation has already been introduced to reduce their emissions. According to the US Environmental Protection Agency (EPA) guidelines, the reduction of chlorinated pollutants can be accomplished through material substitution, product reformulation, process modification and recycling [2]. Many efforts are made to find effective substitutes for the chlorinated solvents but the use of these compounds will continue for years and their disposal/destruction will remain an important ecological problem. The current technology for the total

* Corresponding author. Tel.: +39-41-5298562; fax: +39-41-5298517.

1381-1169/97/$17.00 Copyright © 1997 Elsevier Science B.V. All rights reserved.
PII S1381-1169(96)00287-7

oxidation of the chlorinated organic waste is incineration at extremely high temperatures (> 1000°C), these high temperatures and the construction materials required for the incinerator make this process very expensive. Moreover in this process highly toxic byproducts such as phosgene, formaldehyde, dioxins or dibenzofurans can be produced by incomplete combustion [3]. Catalytic combustion is effective in decomposing chlorinated organics and can be carried out at lower temperatures. This reaction results in water, carbon dioxide and hydrochloric acid. It has been reported that the reaction involves both acid and redox catalysis, so oxides with acidic properties or zeolites were studied as catalysts. Patents claiming complete catalytic oxidation of chlorinated hydrocarbons have appeared in recent years [4]. The reported catalysts can be divided into supported noble metal catalysts and transition metal oxide catalysts (either unsupported or adsorbed onto an inorganic oxide support). The noble metal catalysts (Pd, Pt, Rh, Ru) are not the right choices for deep oxidation because of their high expense and the poisoning of the catalysts by the Cl_2 and HCl produced in the reaction [5–8]. The patents issued for destroying halogenated hydrocarbons with metal oxide catalysts describe systems using a halogenated hydrocarbon concentration typically limited to less than 10000 ppm. Supported transition metal oxides, such as oxides of chromium, manganese, copper, nickel and cobalt and other acidic oxide materials such as zeolites and TiO_2/SiO_2 have also been studied for the total oxidation of chlorinated hydrocarbons [9,7,8,10] but generally they show activity for catalytic combustion. Recently Drago and coworkers reported that CrO_3 supported on a porous carbon is very active for deep oxidation at low temperatures [11]. In a previous paper some of us demonstrated that a natural bentonite pillared with aluminum, aluminum–iron, aluminum–ruthenium and aluminum–chromium polyoxocations resulted active catalyst, to a varying extent, of the deep oxidation of volatile chlorinated hydrocarbons (CVOCs) in the 300–400°C temperature range [12]. Among the aluminum and aluminum doped pillared clays the chromium-doped aluminum pillared clay resulted by far the most active and stable catalyst, with more than 99% hydrocarbon conversion at 300°C. On the other hand, chromia pillared clays have been found to be active in oxidation processes, such as the oxidative dehydrogenation of ethane [13]. The aim of this paper was to study the influence of some of the characteristics of the chromium-based catalysts, such as the acidity, content and oxidation state of chromium, in the deep oxidation of chlorinated hydrocarbons. Two sets of pillared clays were tested, a chromium-doped alumina-pillared clay and three different chromia-pillared clays.

2. Experimental

2.1. Pillared clays syntheses

2.1.1. Materials

The clays used as starting materials were a natural calcium bentonite (Detercal P1) from Nador (Morocco) with unit cell formula $(Si_{7.56}Al_{0.44})(Al_{3.23}Fe_{0.22}Mg_{0.54})O_{20}(OH)_4$ supplied by C. Laviosa SpA (Leghorn, Italy) with a CEC of 85 mequiv/100 g and a Na^+-exchanged montmorillonite from Tidinit (Morocco) with unit cell formula $(Si_{7.94}Al_{0.06})$-$(Al_{2.90}Fe_{0.20}Mg_{0.98})O_{20}(OH)_4$ with a CEC of 125 mequiv/100 g. Chlorhydrol™, a commercial 5/6 basic aluminum chloride salt produced by the Reheis was obtained as a kind gift from Eigenmann and Veronelli (Milan).

The aluminum pillared bentonite APA was obtained by a method described in a previous paper [14]. The chromium doped alumina pillared clay ACrPA was prepared as previously described [12] by adding a solution of Chlorhydrol and $Cr(NO_3) \cdot 9H_2O$ (Al/Cr = 20) to a concentrated suspension (50% w/w) of Detercal P1 in acetone, washing with distilled water and heating in air at 400°C.

The chromium pillared samples XSCr (X = 50, 20, 15 times the CEC of chromium added) were prepared as described [15] by refluxing an aqueous suspension of Na montmorillonite with different amounts of chromium(III) acetate and calcining at 400°C for 4 h in ammonia atmosphere, to avoid Cr^{3+} oxidation.

3. Characterization methods

3.1. Surface area measurement

Adsorption/desorption experiments using N_2 were carried out at 77 K on a C. Erba Sorptomatic 1900. Prior to each measurement the samples were outgassed at 1.33×10^{-3} Pa and at 150°C for six hours. The N_2 isotherms were used to determine the specific surface areas (SA). Surface areas were obtained using the BET equation.

3.2. X-ray diffraction

X-ray diffraction spectra were measured with a Philips PW 1310 diffractometer using the Cu K_α radiation. The samples were disc shaped pressed powders or cast films.

3.3. Analytical determinations

Determination of the chromium content (wt%) was accomplished either by atomic absorption spectroscopy or colorimetrically using the chromate method (λ = 372 nm) after treatment with $NaOH–H_2O_2$.

3.4. XPS analysis

XPS spectra were run on a Vacuum Generator ESCALAB spectrometer, equipped with a hemispherical analyzer operated in the fixed analyzer transmission (FAT) mode, with a pass energy of 20 eV. Al $K_{\alpha_{1,2}}$ and Mg $K_{\alpha_{1,2}}$ photons ($h\nu$ = 1486.6, 1253.6 eV, respectively) were used to excite the photoemission. All the samples were measured as powders pressed on a metal tip or spread on a double-side scotch tape. The binding energy (BE) scale was calibrated by taking the Au 4f7/2 peak at 84.0 eV. Correction of the energy shifts due to static charging of the samples was accomplished by referencing to the Al 2p peak from the support taken at 74.7 eV. The accuracy of the reported BEs is ± 0.2 eV. The spectra were collected by a DEC PDP 11/83 data system and processed by means of a VGS 5200 data handling software.

3.5. Temperature programmed reduction

Temperature programmed reduction (TPR) was performed in a conventional U-shaped quartz microreactor (bore = 6 mm, length = 200 mm) using a 5% H_2/Ar mixture flowing at 35 ml min^{-1} (STP). The temperature range was 25–700°C and the heating rate 10°C min^{-1}. The reduction of CuO to metallic copper was used to calibrate the TPR apparatus for H_2 consumption.

3.6. Temperature programmed desorption

TPD of ammonia was used to determine the total acidity of the samples. Before the adsorption of ammonia at 100°C, the samples were heated at 400°C in He flow.

The ammonia TPD were determined between 100 and 400°C, at 10°C min^{-1}, and analyzed by on line gas chromatography (Shimadzu GC-14A) provided with a thermal conductivity detector.

3.7. Catalytic 1-butene isomerization test

Catalytic 1-butene isomerization tests were performed in a tubular glass flow microreactor. Catalyst samples (250 mg) were pretreated for 2 h in N_2 flow at 400°C. Experiments were performed at $\tau = 2.4\, g_{cat} \cdot g^{-1}_{1\text{-butene}} \cdot h$. The 1-butene was at 5% in nitrogen and the time on stream was 120 min. All the catalysts were tested for a total of 240 min of time on stream.

The amount of coke has been deduced from the weight loss of the spent catalyst during burning in air in the range 90–800°C, measured by thermogravimetry (TG).

3.8. Catalytic deep oxidation measurements

The deep oxidation reactions were carried out in a tubular stainless-steel flow reactor interfaced to a gas chromatograph (HP 5890) equipped with FI and TC detectors. Methylene chloride was vaporized into the carrier gas stream (He) using a thermostated saturator. Typical experiment conditions: 500 mg of clay, total flow of reactants (air and chlorinated hydrocarbon in helium) = 90.0 ml/min, chlorinated hydrocarbon concentration 10000 ppm, and total pressure = 101.3 kPa, (space velocity = 12000 h^{-1}). The reaction was monitored determining the remaining chlorinated hydrocarbon by GC with a 25 m wide bore column 50% PhenylMethyl Silicone working at 120°C with a carrier gas flow of 10 ml/min. The formation of CO and CO_2 was periodically determined by GC. Hydrochloric acid was determined by titration. Partial oxidation products (phosgene and formaldehyde) and chlorine (formed by the Deacon reaction) were never found by usual detection methods.

4. Results

4.1. Characterization of pillared clays

Metal content, basal spacing values, and surface area of the PILCs are summarized in Table 1. The basal reflection $d(001)$ of the samples prepared by two methods were in the range 1.44–1.82 nm, and the surface area are all within 333.0 and 388.5 m^2/g. The significant differences in the preparation conditions between chromia pillared montmorillonites 'XSCr' (where X is 50, 20 or 15) and chromium doped alumina pillared clay (ACrPA) are reflected by the difference in chromium content. APA is an alumina pillared bentonite [14].

Table 1
Metal content, X-ray, and surface areas of the pillared clays

	Cr% (w/w)	d_{001} (nm)	S.A. (m^2/g)
APA	—	1.82	388.5
ACrPA	1.3	1.82	350.2
50SCr	21.1	1.44	349.0
20SCr	19.2	1.52	353.0
15SCr	18.2	1.53	333.0

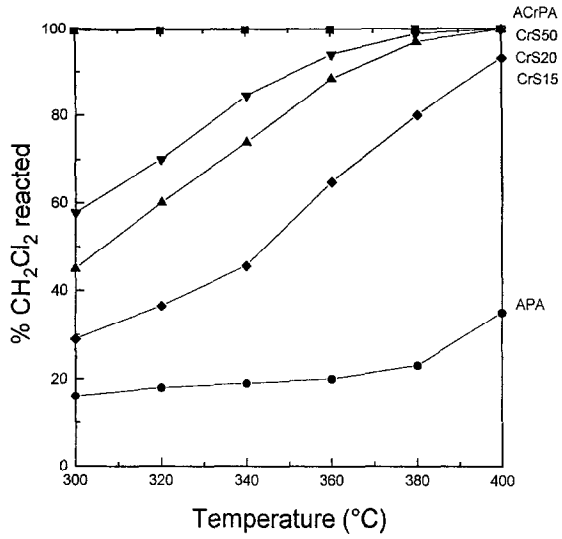

Fig. 1. Deep oxidation of CH_2Cl_2 on the pillared clays.

4.2. Catalytic deep oxidation measurements

The behavior of the pillared clay catalysts in the dichloromethane deep oxidation in the 300–400°C temperature range is shown in Fig. 1.

Methylene chloride was chosen as substrate for the oxidation because it is one of the more refractory halocarbons. It is known, in fact, that halocarbons with carbon–carbon linkages or higher numbers of halogen atoms can be destroyed at lower temperatures.

All the catalytic reactivity data were obtained after reaching the steady state conditions (typically 1 h).

Both ACrPA and almost all XSCr clays showed a good activity (conversion > 80%) at temperature > 350°C. However only the

Al/Cr-pillared clay (ACrPA) was still active with more than 99% hydrocarbon conversion at 300°C. The APA reference clay, a highly porous and acidic aluminum pillared clay, was almost inactive (conversion < 30%) in the 300–400°C temperature range.

4.3. XPS measurements

XPS analysis of the clay surface before and after the title reaction showed that the chromium atoms of APCrA and *X*SCr (Table 2) were in different oxidation states.

The Al–Cr-pillared clay (ACrPA) showed a broad Cr 2p peak at 579.2 ± 0.2 eV. This BE value can be attributed to Cr^{6+} ions [16] while the chromium pillared clays '*X*SCr' showed a Cr 2p peak at 576.7 ± 0.2 eV that can be attributed to the Cr^{3+} ion [16]. No changes in the binding energy values of all the pillared clays were observed after 72 h of reaction.

The chromium content of the ACrPA sample was found unchanged after the catalytic experiments while a significant decrease of the Cr/Si ratio was detected for the Cr-pillared clays after the reaction.

4.4. TPR analysis

TPR analysis has been largely used to study supported mono and bimetallic catalysts [17,18]. Metal oxides supported on inert carriers such as γ-Al_2O_3 or SiO_2 and unsupported oxides may exhibit different reduction behaviors. Metal oxides dispersed on pillared clays may be homogeneously distributed on the surface of the support or exist as islands of oxide within the pore structure, or may be incorporated into the structure of the pillar.

Table 2
Binding energies (eV) and XPS atomic ratios for the reported compounds. All binding energies are referenced to the Al 2p peak taken at 74.7 eV

	BE Cr $2p_{3/2}$		Cr/Si (atomic ratio)		Si 2p
	before	after	before	after	
ACrPA	579.2	579.2	0.04	0.04	102.5
50SCr	576.6	576.9	1.41	0.32	102.5
20SCr	576.7	576.7	0.78	0.29	102.5
15SCr	576.6	576.7	0.60	0.24	102.5

BE Cr $2p_{3/2}$ reference value: CrO_3 580.1; $CrCl_3$ 577.8; Cr_2O_3 576.6; Cr_{met} 574.3. The accuracy of the reported BEs is ±0.2 eV.

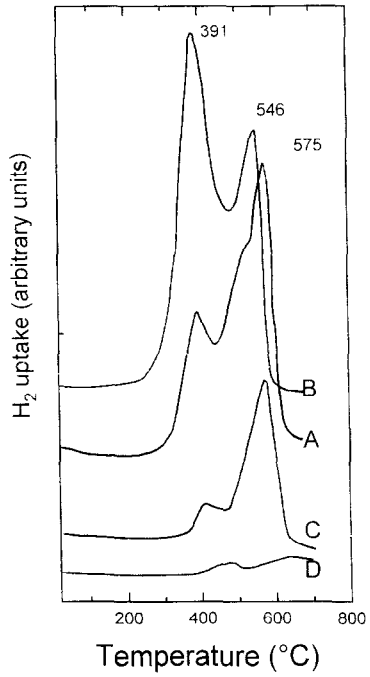

Fig. 2. H_2-TPR profile in the range 20 ÷ 700°C for the reported clays.

Temperature programmed reduction of pillared clays can be an useful method to prove the isomorphic substitution in the pillars [19–21].

The TPR experiments on ACrPA are described in Fig. 2. As shown in Fig. 2 (curve D), no H_2 consumption peak was observed for the aluminum-reference pillared clay APA, in the same temperature range. Curve A is the TPR profile of the ACrPA clay as prepared, treated with H_2 (5% in Ar) up to 700°C. The curve showed an intense TPR peak centered at 391°C, a shoulder at 546°C and a peak centered at 575°C. The reduced clay from the first experiment was oxidized in air flow at 400°C before the second experiment described by curve B. The curve had two peaks respectively centered at 391°C and 546°C.

Table 3
TPD of ammonia in the range 100 ÷ 400°C over the pillared clays

	Ac. tot. (μmol NH_3/g)	100–200°C	200–300°C	300–400°C
APA	697.0	111.8	262.5	322.3
ACrPA	1056.3	143.7	414.8	497.8
50SCr	862.0	90.8	402.0	369.0
20SCr	653.0	141.0	288.0	224.0
15SCr	716.9	87.5	312.0	317.4

The spent ACrPA catalyst showed a behavior identical to that shown by the fresh one. Curve C is the TPR profile of an ACrPA sample measured after washing with distilled water to remove the only adsorbed chromium(VI). An intense hydrogen uptake peak at 575°C was observed along with another very small peak at lower temperature (400°C).

4.5. Acidity evaluation

Temperature-programmed desorption of ammonia is probably, with the possible exception of FT-IR measurements of adsorbed pyridine, the most widely used method to study zeolites and PILCs acidity. The amount of ammonia desorbed at some characteristic temperatures is taken as a measure of the acid sites concentration while the temperature range in which most of ammonia was desorbed indicates the strength of the acid sites. The total acidity and the acid strength distribution of all the samples, determined as described in the experimental section by TPD of ammonia, are presented in Table 3.

The total acidity values are comparable to those found for analogous compounds [21]. It clearly appears from the obtained data that the total acidity of the ACrPA sample was higher than that of all the other samples. Moreover NH_3 resulted to desorb from the ACrPA sample at higher temperature indicating that its acid sites were stronger than those of the *X*SCr clays.

To further investigate the acidity of the clay samples, the catalytic 1-butene isomerization was chosen as test reaction [22–24].

The product distribution of 1-butene conversion over all the catalysts are summarized in Table 4.

The reaction products can be divided into the following groups: (a) double bond isomerization products (*cis*-2-butene and *trans*-2-butene); (b) skeletal isomerization products (isobutene); (c) hydrogenated products (*n*-butane and isobutane); (d) cracking products (methane, ethane, ethylene, propane and propene (C4 −); (e) surface carbon residues; (f) butadiene and higher molecular weight compounds (C4 +).

It was reported that the formation of isobutene (skeletal isomerization) needs stronger Brønsted acid sites ($H_R < -6.63$) than those required by the geometric isomerization and the double bond migration ($0.82 > H_R > -4.04$) [22–24]. The reaction is thought to occur on Brønsted acid sites via carbenium ion intermediates by a three-step mechanism: protonation of the reactant, rearrangement of the carbenium ion formed, desorption of the products, with the rearrange-

Table 4
Product distribution in 1-butene conversion at 400°C on the pillared clays

	iso-bu (%)	*n*-bu (%)	*trans*-2bu= (%)	1-bu= (%)	*iso*-bu= (%)	*cis*-2bu= (%)	C4 − (%)	*iso*-tot (%)
APA	3.7	1.5	28.9	21.7	16.7	22.6	4.3	20.4
ACrPA	0.7	1.8	34.9	25.1	8.0	26.6	2.0	8.7
50SCr	0.1	0.1	38.1	24.8	6.2	29.5	1.0	6.3
20SCr	0.0	0.2	38.8	24.7	5.8	29.7	0.8	5.8
15SCr	0.1	0.2	38.7	24.6	6.1	29.6	0.7	6.2

iso-bu (isobutane); *n*-bu (*n*-butane); *trans*-2bu= (*trans*-2-butene); 1-bu= (1-butene); *iso*-bu= (isobutene); *cis*-2bu= (*cis*-2-butene); C4 − (methane, ethane, ethylene, propane and propene); *iso*-tot (isobutane + isobutene). $T = 400$°C; $\tau = 2.4\, g_{cat} \cdot g^{-1}_{1\text{-butene}} \cdot h$; time on stream = 120 min.

ment being the reaction rate limiting step. The isobutene yield is limited by several parallel or consecutive reactions. The hydrogenated C_4-compounds *n*-butane and isobutane were found among the other products. These compounds are usually generated by butene cracking and their presence can be explained by a cracking reaction of butene oligomeric carbenium ions or alternatively, by a direct hydrogenation of the butene isomers through hydride transfer on the corresponding monomeric carbenium ions.

In order to have an idea of the skeletal isomerization activity of the clays the amount of isobutene produced should be added to isobutane, assuming that isobutane originates from isobutene.

As shown in Table 4 the ACrPA pillared clay was much more active in the skeletal isomerization, that needs stronger Brønsted acid sites (isobutene and isobutane formation), than the *X*SCr-pillared clays. Moreover the ACrPA pillared clay produced more *n*-butane and isobutane, C4 − compounds, and surface carbon residues. Coke formation was investigated after 4 h on stream. The ACrPA sample was found to produce 1.3 wt% of coke, whereas all the other chromium pillared clays contained after 4 h of reaction a negligible quantity of carbonaceous compounds.

5. Discussion

It is known that chromium based catalytic systems are very active in the CVOCs deep oxidation reaction in the 300–400°C temperature range [8,10,11] and the effectiveness of Cr-doped Al PILCs was demonstrated in a previous work [12].

The catalytic activity of ACrPA and *X*SCr resulted quite different. The active metal oxidation state must be at least in part responsible of this behavior.

The chromium doped aluminum montmorillonite clay (ACrPA) was prepared by adding a Cr^{3+} salt to the solution of aluminum Al_{13} oligomer. Some of the chromium(III) is presumed to be incorporated into the structure of the Keggin ion Al_{13}, $[Al^{IV}(Al_{12-x}Cr_x)^{VI}O_4(OH)_{24}]^{7+}$ ($x = 1, 2, 3$), by isomorphic substitution of the octahedral aluminum and some can be only adsorbed on the surface. Cr(III) must be subsequently oxidized to Cr(VI) during the PILC calcination in air. It is known that Cr(VI) compounds are unstable at high temperatures in deep oxidation conditions and easily reduced to Cr(III), nevertheless Cr(VI) centers of ACrPA appeared not to be reduced during the catalytic reaction between 300 and 400°C, as demonstrated by XPS data. In contrast *X*SCr chromia pillared samples were prepared by calcination under a reducing NH_3 atmosphere, to avoid Cr^{3+} oxidation. In this case, the observed values of the binding energies are typical of Cr_2O_3 both before and after the reaction. Nevertheless as the Cr $2p_{3/2}$ peak of the ACrPA clay is very broad, in order to more precisely identify the nature and the oxidation state of the chromium centers, the sample was studied by H_2-TPR (Fig. 2). Curve B shows the H_2-TPR behavior of the ACrPA sample after reduction at 700°C and subsequent reoxidation in air flow at 400°C. The thermal treatment at 700°C is known to lead to the collapse by of the PILC tridimensional structure with segregation of the chromium eventually present in the pillars. All the metal was reoxidized to Cr(VI) by treatment in air at 400°C. Therefore the two peaks centered at 391°C and 546°C (curve B) must correspond to the Cr(VI) to Cr(III) and Cr(III) to Cr(II) reduction steps of Cr(VI) dispersed on an silica–alumina surface. On the other hand, the TPR profile of ACrPA pillared clay (Fig. 2, curve A), both before and after the title reaction, showed a Cr(VI)/Cr(III) reduction peak centered at 391°C, and a Cr(III)/Cr(II) reduction peak centered at 575°C with a shoulder at 546°C. The TPR behavior of a series of Cr/Al pillared montmorillonite samples with Cr/Al ratios ranging from ∞ to 0.2 was reported by Zhao et al. [21]. It was observed that the position of the Cr(III)/Cr(II) peak moved from 484 to 572°C

as the Cr/Al ratio decreased. The authors suggested that at low Cr/Al ratios (< 0.1) the Cr was highly dispersed in the 'chromalumina' [25] pillars and more difficult to reduce in analogy with what is found for other bimetallic systems [19,20].

The fact that the high temperature peak was more intense than that at low temperatures suggests that the initial sample contains Cr(III) and Cr(VI), the former probably as a vicarious ion of the octahedral Al(III) of the pillars, and the latter as an extra-framework species. It was reported that a low Cr/Al ratio (0.05) of the pillaring solution lead to the synthesis of samples where the chromium atoms were present only as components of the mixed metal pillars [20,21], but the Al–Cr substitution appears to have occurred only in part with the synthetic procedure used. To confirm this hypothesis a sample of ACrPA was washed with water to elute the adsorbed Cr(VI) species, filtered, air dried and reduced in TPR conditions. The TPR profile of the treated as above described sample is shown by curve C. The presence of a main reduction peak at 575°C confirmed the presence of Cr^{3+} in the initial samples. Thus, some Cr^{3+} may be incorporated in the alumina pillars which is not oxidized at high temperatures.

Both ACrPA and *X*SCr chromium pillared clays showed a good activity at temperatures > 350°C, but only the Al/Cr-pillared clay (ACrPA) was still active with more than 99% hydrocarbon conversion at 300°C.

No loss of chromium was detected during the catalytic experiments with ACrPA while a significant decrease of the Cr/Si ratio of the *X*SCr clays after the reaction was found. Nevertheless the stability of all the catalysts was checked after 72 h of reaction at 400°C and no apparent loss of activity was observed. Therefore the chromium loss observed for *X*SCr catalysts must have occurred, as reported for commercial chromium based deep oxidation catalysts [26], probably by the formation of the volatile CrO_2Cl_2 during the initial reaction stage. This finding suggests that in the *X*SCr samples some chromium(III) was present as easily removable oxide deposited on the clay surface and some as highly polymerized constituent of the pillars that prop open the clay layers.

It was reported [8,10,11] that both Cr(III) and Cr(VI) can catalyze CVOCs deep oxidation at high temperatures, but most likely only Cr(VI) is the active metal oxidation for the low-temperature reaction. Chromium(VI) species are known to be unstable in the total oxidation reaction conditions and the unusual high stability of ACrPA pillared clay was probably due, as proposed for other Cr-based active catalytic systems [8,10,11], to the high metal dispersion and to the presence of stabilized mixed-valent Cr(VI)–Cr(III) species. The ACrPA catalytic system can tentatively be described as adsorbed Cr(VI) species on Al^{3+}/Cr^{3+} mixed oxide pillars while the active sites of *X*SCr are in the Cr(III) oxide pillars. Both the acidity and the metal oxidation state of the two chromium based systems appear to be important in determining the catalytic activity.

It was proposed that catalysts based on Cr(VI) on a carbonaceous support function via a non-oxidative pathway, while the carbon itself functions in a net oxidative manner [10]. Nevertheless we found that the Al pillared clay APA was only a very poor catalyst. The generally proposed deep oxidation mechanism model of methylene chloride involves, in a probable multi-step process, adsorption of the hydrocarbon on Brønsted acid sites and of oxygen on metal ion sites [7]. Both ammonia TPD measurements and 1-butene isomerization data obtained suggested that ACrPA has more and stronger Brønsted acid sites when compared to *X*SCr chromium-pillared clays.

As shown in a previous paper [12] the activity of a bifunctional catalyst appears to depend on a delicate balance of the two active functions.

There is a general agreement to locate the Lewis acidity sites of an Al pillared in the clay pillars [27–30] while the location of Brønsted sites is more controversial. It was proposed that

PILCs Brønsted acid sites are dependent on the parent clay and are situated part on the pillars and part on the tetrahedral layer [27–30]. It is also widely accepted that transition metal ions added as dopants to the pillaring solution modify the pillar chemical composition and consequently the strength and nature of the acid sites [20,21,25,31,32]. Moreover precedence for Cr(VI) functioning as a Lewis acid in a non-oxidative process is seen in the reaction of CrO_3 with HCl to form $HOCrO_2Cl$ and CrO_2Cl_2 [33]. The ACrPA sample showed a high total acidity and the acid sites were stronger than the *X*SCr-pillared clays as most of the NH_3 desorbed at higher temperatures. This is consistent with what is found when measuring the acidity of some pillared clays prepared with solutions containing various atomic ratios of Cr and Al [21].

As shown in Table 4, ACrPA was much more active than the *X*SCr in the butene skeletal isomerization, that require stronger Brønsted acid sites. Furthermore ACrPA yield more C4-compounds, *n*-butane and isobutane and surface carbon residues indicating the presence of strong Lewis acid sites [34]. The negligible quantity of coke detected on the chromium pillared clays after 4 h on stream suggests the presence mainly of Brønsted acid sites, as found by other authors for a chromium pillared montmorillonite treated at 400°C [32].

We can tentatively conclude that the ACrPA catalytic activity, apparently independent from the temperature, is attributable, analogously to what found for similar systems [8,10,11], to the presence of a Cr(VI)/Cr(III) stabilized species in the clay cavities that influence both the acidity and the redox properties. The catalytic species was most probably the strictly interacting system formed by Cr(VI) species adsorbed on the mixed metal pillars. The Cr(III) signal was not detected by the XPS or because of the poor quality of the spectrum or because the Cr(III) atoms were below the explored sample layer.

The catalytic activity of the *X*SCr samples resulted in the increase of the Cr content, indicating that the acid sites are located on the chromia pillars. Nevertheless trivalent chromium oxide is known to be less reactive and good activity was observed only at high temperatures as observed for other systems [12].

Acknowledgements

The financial support of M.U.R.S.T. (ex quota 40%) and of CNR (Progetto Strategico and Comitato 11) is acknowledged. The authors thank A. Talon for the analytical determinations. This research was also supported by the CICYT (Spain) Project MAT94-0678 and E.U. Programme BRITE-EURAM, Contract BRE2-CT93-0450.

References

[1] D. Hanson, Chem. Eng. News March 12 (1990) 4; March 29 (1993) 7; B. Hileman, Chem. Eng. News April 19 (1993) 11.
[2] L.R. Ember, Chem. Eng. News July 8 (1991) 7.
[3] J. Josephson, Environ. Sci. Technol. 18 (1984) 222A.
[4] T.L. Wolford, U.S. Patent No. 4,423,024, Dec. 27, 1983; D.A. Livingston and J.P. Surls, U.S. Patent No. 4,587,116, May 6, 1986; A.D. Harley, U.S. Patent No. 4,816,609, March 28, 1989; T. Dockner, M. Sauserwald, H. Krug and M. Irgang, U.S. Patent No. 4,943,671, July 24, 1990.
[5] P. Subanna, H. Greene and F. Desal, Environ. Sci. Technol. 22 (1988) 557.
[6] S.L. Hung and L.D. Pfefferle, Environ. Sci. Technol. 23 (1989) 1085.
[7] S. Chatterjee and H.L. Greene, J. Catal. 130 (1991) 76; S. Chatterjee, H.L. Greene and Y. Joon Park, J. Catal. 138 (1992) 179.
[8] S.C. Petrosius and R.S. Drago, J. Chem. Soc. Chem. Commun. 344 (1992).
[9] S. Imamura, H. Tarumoto and S. Ishida, Ind. Eng. Chem. Res. 28 (1989) 1449.
[10] S.C. Petrosius, R.S. Drago, V. Young and G.C. Grunewald, J. Am. Chem. Soc. 115 (1993).
[11] M.L.H. Green, R.M. Lago and S.C. Tsang, J. Chem. Soc. Chem. Commun. 365 (1995) 6131.
[12] L. Storaro, R. Ganzerla, M. Lenarda and R. Zanoni, J. Mol. Catal. A 97 (1995) 139.
[13] P. Olivera-Pastor, J. Maza-Rodriguez, A. Jiménez-Lòpez, A. Guerrero-Ruìz and J.L.G. Fierro, in: Studies in Surface Science and Catalysis 82, New Developments in Selective Oxidation II, V. Cortés Corberàn and S. Vic Bellòn (Eds.) (Elsevier Science, B.V., Amsterdam, 1994) p. 103.

[14] L. Storaro, R. Ganzerla, M. Lenarda and A. Rinaldi, Microporous Mater. 6 (1996) 55.
[15] A. Jiménez-López, J. Maza-Rodríguez, P. Olivera-Pastor and E. Rodríguez-Castellón, Clays Clay Miner. 41 (1993) 328.
[16] F. Capece, V. Dicastro, C. Furlani, G. Mattogno, C. Fragale, M. Gargano and M. Rossi, J. Electron Spectrosc. Relat. Phenom. 27 (1982) 119.
[17] N.W. Hurst, S.J. Gentry, A. Jones and B.D. McNicol, Catal. Rev. Sci. Eng. 24 (1982) 233.
[18] A. Jones and B.D. McNicol, Temperature Programmed Reduction for Solid Materials Characterization (Marcel Dekker, New York, 1986).
[19] F. Bergaya, N. Hassoun, J. Barrault and L. Gatineau, Clay Miner. 28 (1993) 109.
[20] D. Zhao, G. Wang, Y. Yang, X. Guo, Q. Wang and J. Ren, Clays Clay Miner. 41 (1993) 317.
[21] D. Zhao, Y. Yang and X. Guo, Zeolites 15 (1995) 58.
[22] A. La Ginestra, P. Patrono, M.L. Berardelli, P. Galli, C. Ferragina and M.A. Massucci, J. Catal. 103 (1987) 346.
[23] P. Patrono, A. La Ginestra, G. Ramis and G. Busca, Appl. Catal. A 107 (1994) 249.
[24] J.P. Damon, B. Delmon and J.M. Monnier, J. Chem. Soc. Faraday Trans. I 73 (1977) 372.
[25] M.S. Tzou, T.J. Pinnavaia, Catal. Today 2 (1988) 243.
[26] P. Manning, Hazardous Waste 1 (1984) 41.
[27] M.L. Occelli and R.M. Tindwa, Clays Clay Miner. 31 (1983) 22; M.L. Occelli and J.E. Lester, Ind. Eng. Chem. Prod. Res. Dev. 24 (1985) 27.
[28] D. Plee, A. Schutz, G. Poncelet and J.J. Fripiat, in: Catalysis by Acids and Bases, B. Imelik, C. Naccache, G. Goudurier, Y. Ben Taarit and J.C. Vedrine (Eds.) (Elsevier, Amsterdam, 1985) p. 343.
[29] D. Tichit, F. Fajula, F. Figueras, J. Bousquet and C. Guegen, in: Catalysis by Acids and Bases, B. Imelik, C. Naccache, G. Goudurier, Y. Ben Taarit and J.C. Vedrine (Eds.) (Elsevier, Amsterdam, 1985) p. 351.
[30] G. Poncelet and A. Schutz, in: Chemical Reactions in Organic and Inorganic Constrained Systems, R. Setton (Ed.) (Reidel, Dordrecht, 1986) p. 165.
[31] K.A. Carrado, S.L. Suib, N.D. Skoularikis and R.W. Coughlin, Inorg. Chem. 25 (1986) 4217.
[32] J. Jamis, A. Drljaca, L. Spiccia and T.D. Smith, Chem. Mater. 7 (1995) 2078.
[33] F.A. Cotton and G. Wilkinson, Advanced Inorganic Chemistry (John Wiley and Sons, New York, 1988).
[34] J. Datka, J. Chem. Soc. Faraday Trans. I 77 (1981) 2633.